PHYSICAL REVIEW B VOLUME 17, NUMBER 12 15 JUNE 1978

Angle-resolved photoemission from molecules in the independent-atomic-center approximation

Warren D. Grobman
IBM Thomas J. Watson Research Center, Yorktown Heights, New York 10598
(Received 19 October 1977)

This paper considers several implications of the approximation that the total amplitude for photoemission from an oriented molecule is the sum of the amplitude of coherent emission from spherically symmetric regions at the atomic centers. We show that this approximation, which is increasingly valid at high energies (accessible, for example, to synchrotron-radiation sources) is readily calculable using tabulated initial-state atomic functions and simple solutions of the radial Schrödinger equation. We illustrate the fact that in special but important cases (e.g., oriented benzine), one can obtain the angular distribution of photoemission at fixed final energy without any recourse to atomic-photoemission-amplitude calculations. Finally, we emphasize that fact that the orthogonalized-plane-wave approach, which is a special case of the independent-atomic-center approximation, fails in two regards—neglect of atomic phase shifts, and the neglect of initial-state core-region wave-function behavior, which is crucial at high energies. This latter point is illustrated by comparing orthogonalized-plane-wave calculations using Slater atomic functions (which emphasize the bonding-region wave-function behavior), and hydrogenic wave functions, which can have radial nodes and core-region behavior which can more closely approximate the behavior of the true initial-state wave functions.

I. INTRODUCTION

Understanding the angular distribution of photoelectrons emitted from a particular molecular orbital of an oriented molecule is of great interest for two fundamental reasons. The first is that a theory of this process can be used to predict the angular distribution of photoelectrons from an orbital of a molecule in the vapor phase, and can be used as a powerful tool for associating photoemission peaks at particular binding energies with molecular orbitals of a given symmetry. Second, the angular distribution of photoemission from an orbital of a molecule adsorbed on a surface contains, in principle, information concerning the orientation of the molecule on the surface—information of fundamental importance in surface chemistry.

The main idea of this paper is to calculate oriented-molecule photoemission amplitudes in a model in which emission from the individual atomic centers of the molecule occurs *independently* (but *coherently*). Such an *independent-atomic-center* (IAC) approximation is rather widely represented in the literature, for the many papers using a linear-combination-of-atomic-orbitals (LCAO) initial state and a plane-wave (PW) or orthogonalized-plane-wave (OPW) final state are of this class.[1-6] The great advantage of a model of this type is that it represents an attractive alternative to low-energy electron diffraction (LEED) as a tool for surface-structure determination.[7] This paper will derive several results which, at large photon energy $h\nu$ (accessible with synchrotron radiation or an x-ray photoemission spectrometer) are of a particularly simple form which can be easily calculated and used as a guide by experimentalists. This is due to the dominance at large $h\nu$ of something similar to a diffraction pattern emitted by the molecule as its independent emitting centers coherently interfere. This dominance of *geometrical* rather than *atomic* features at large $h\nu$ is one of the central themes of this paper.

What is new in this paper occurs in two areas of major emphasis. One is a rather general formulation of the problem which permits the atomic photoemission matrix elements (which contribute to the final molecular-orbital emission amplitude) to be calculated much more precisely than is done in the very commonly used OPW and PW approximations. These make errors both in the magnitude of the atomic-emission amplitudes, and in their phase, which is fixed at large distances by the OPW and PW phases.

The second area of general emphasis in this paper is our detailed discussion of the contribution of two types of factors that arise in the expression for the total amplitude in IAC approximations. One type of factor is the angle-resolved amplitude from individual atomic orbitals, while the second type is a geometrical factor, alluded to above, which is much simpler to calculate.[8] We discuss the fact that the relative importance of these two types of factor changes dramatically as one increases the final-state kinetic energy (or the photon energy $h\nu$). In particular, at large $h\nu$ one enters a regime where the rather simply calculated geometrical factors, rather than the atomic factors, produce the most dramatic (sharpest in angle) structure in the angle-resolved photoemission intensity.

In the case of an adsorbed molecule, the angular distribution of photoemitted intensity has two contributions. One is direct emission from the molecule to the detector, while the second consists of backscattered electrons which are emitted by the molecule toward the substrate, and then scatter toward the detector.[9-13]

The present paper, in calculating the direct emission from a molecule to a detector ignores the effect of the substrate on the angular distribution. However, it provides the first step toward understanding substrate effects, for it is the emission from the adsorbed molecule toward the surface which provides the ultimate source of the scattered wave.

We contrast this calculation with several recent ones, based on LEED theory, which have been interested in the limit in which the photoemitting center itself is very simple (e.g., an s orbital of a single adsorbed atom) and *all* of the angular complexity is due to substrate scattering.[9-13] We are treating the opposite limit, one in which the emitting, adsorbed species is one of complex geometrical structure, with an angular distribution rich in structure in its direct photoemission amplitude to the detector.

Another main feature distinguishes the current work from some recent calculations. In these the system of interest is a single atom which is chemisorbed on a surface, forming new bonds (to the surface) with a particular symmetry dependent on the adsorption site. Our calculation assumes weak chemisorption of covalent molecules, so that the initial state in the photoemission process is in zeroth order an unperturbed molecular orbital of the free molecule. Such an approximation is amply justified by the close correspondence between photoemission spectra of vapor phase and adsorbed molecules of a particular species.[14]

This correspondence is illustrated for the case of condensed CH_3OH on Pd (Fig. 1) which shows that the spectral form of the *extra emission* due to the adsorbed species is related to that of the vapor-phase molecule, with energy shifts, however, due to relaxation-polarization effects and a bonding shift of the highest-lying orbital. In the case of oriented, adsorbed molecules, our interest in this paper is in understanding the dependence of the *extra emission* δI [denoted $\Delta N(E)$ in Fig. 1] due to the adsorbed molecule as a function of detector *direction* $\hat{R}$ for fixed $h\nu$. This is in strong contrast to the case where δI at fixed angle is determined as a function of $h\nu$. In this case $\delta I(\hat{R}, h\nu = \text{const})$ might contain much multiple scattering (from the substrate) background whose angular dependence is either not strong or is of a different symmetry from that due to direct molecular emission. Our neglect of substrate multiple scattering in that case still permits identification of features in δI vs $\hat{R}$ as due to molecular orientation. Another type of measurement $\delta I(\hat{R} = \text{const}, h\nu)$ is possibly much more sensitive to substrate backscattering. That is, even if the angular form of substrate backscattering does not complicate the pattern due to direct molecular emission, the photon-energy-dependent strength of such scattering may vary strongly[15-17] with changing $h\nu$. For this reason $\delta I(\hat{R} = \text{const}, h\nu)$ is in some way similar[7] to a LEED "I-V plot," and is not of interest in this paper.

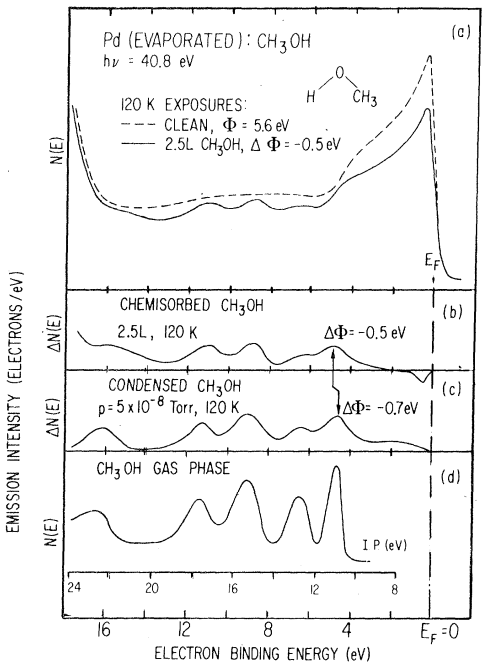

FIG. 1. Subtraction of the photoemission spectrum of clean Pd (dashed) from that of Pd plus chemisorbed CH_3OH in (a) yields the curve (b) the extra emission due to the adsorbed molecules. Curve (c) is similarly the extra emission due to condensed CH_2OH, while (d) is that of the free molecule. Φ is the work function, I.P. is the ionization potential. This figure illustrates a fact discussed by many authors (e.g., see Ref. 14)—the emission spectrum of the adsorbed covalent molecule is nearly the same as that of the free molecule. [This figure has been obtained from H. Luth, G. W. Rubloff, and W. D. Grobman, Surf. Sci. 63, 325 (1977)].

A recent approach for calculating $\delta I(\hat{R}, h\nu = \text{const})$, based on multiple-scattering theory, is an X_α transition-state calculation which was used to obtain the angular distribution of photoemission from an oriented molecule.[18] An application of this method to the case of photoemission from CO has recently been described, and offers the advantage of describing final-state multiple scattering in some detail, which our present method does not.

However, especially for organic molecules which are somewhat larger than CO, the X_α method provides a much poorer description of the *initial-state* wave function than does the present method. Thus, especially for larger molecules, and for high enough final-state energy that multiple scattering is somewhat weaker than the direct emission from the individual atomic centers, the approximation used here may offer significant advantages compared with the X_α approach.

The formalism for describing molecular photoemission is developed in Sec. II. In order to make contact with previous papers based on the PW and OPW methods, and in order to illustrate that these are examples of an IAC approximation, we first rederive in Sec. II A the OPW and PW expressions for photoemission from an LCAO molecular orbital. Section II B then derives the IAC approximation in a formal manner in which we emphasize particularly that a much more accurate result is obtained if the atomic matrix elements which appear are determined in terms of final-state wave functions which are solutions of the Schrödinger equation in the atomic potential of the emitting center, rather than the *ad hoc* final state used in the PW and OPW approximations.

Three applications of the IAC method are described in Sec. III. One of these is an illustration of the manner in which, at high final-state energies, the result one calculates is dominated by something like a "diffraction pattern" from the radiating molecule. This model calculation relies on OPW and PW matrix elements. A second application is to the case of π orbitals of benzene, in which we illustrate the manner in which one can calculate exact yet totally geometry-dependent results in particular cases—exact results which do not even require calculation of the atomic transition factors, which do not enter the final result if detector directions, molecular orientation, and light polarization are suitably chosen. A third application of the method, again a model calculation based on the OPW final-state wave function, illustrates the application of the IAC method to the calculation of vapor-phase β factors. Finally, in Sec. IV, we discuss these results, as well as presenting several general conclusions.

II. FORMALISM FOR MOLECULAR PHOTOEMISSION

This section will derive the basic equations which represent molecular photoemission determined from a sum of emission amplitudes from separate atomic orbitals. We will first rederive in our notation the orthogonalized-plane-wave final-state approach as used, for example, in Refs. 1–6. The resulting formulas then lead in a natural way to the basic equations of the general independent atomic center method we wish to describe in this paper Further, the OPW (or plane wave) approach is then seen to be an approximate version of the IAC method. For this reason OPW results can be used later in this paper in order to illuminate some of the general qualitative features which would be exhibited by the IAC method if a calculation were performed based on correct final-state atomic wave functions.

A. Orthogonalized-plane-wave and simple-plane-wave approaches

The starting point for this calculation is the representation of the ith occupied molecular orbital (initial state) wave function $\psi_i(\vec{r})$ as a linear combination of atomic orbitals

$$\psi_i(\vec{r}) = \sum_\alpha C_{i\alpha}\varphi_\alpha(\vec{r} - \vec{R}_\alpha) \ . \tag{2.1}$$

In Eq. (2.1), $\varphi_\alpha(\vec{r} - \vec{R}_\alpha)$ is an atomic orbital centered on the atom whose ion core is at $\vec{R}_\alpha$, and α represents the principal and angular-momentum quantum numbers as well as the atomic center on which the orbital resides.

At this point we emphasize a fundamental difference between the use of Eq. (2.1) by previous authors who have used the OPW method[1-6] and the present paper. As others have done, we will get the atomic orbital coefficients $C_{i\alpha}$ from a molecular-orbital calculation (Gaussian-70 for this paper)[19] which uses the Hartree-Fock-Roothan method in which the total molecular wave function is a Slater determinant of molecular orbitals of the form of Eq. (2.1) with the φ_α represented by Gaussian functions. However, for calculating photoionization cross sections, we will then *replace* the φ_α in Eq. (2.1) with atomic orbitals whose behavior at small r more properly represents true Hartree-Fock atomic wave-function behavior near the core. The main point is that the form of the φ_α in Eq. (2.1) required for a molecular-orbital calculation should be rather accurate in the bond region, at rather large r, in order to obtain proper values for the $C_{i\alpha}$ and the related molecular chemistry information (density and bond order matrices, total binding energy, etc.). However, when one then changes the quantity of interest to photoionization at high photon energies, which is the thing of interest in this paper, one must replace the φ_α in Eq. (2.1) by atomic functions whose form ensures approximately correct atomic cross sections over a wide energy range. *Such a replacement is a fundamental difference between the present work and previous calculations based on the OPW method.*

For the final-state wave function $\Psi_E(\vec{r})$ in the OPW approximation, denoted by $f_{\vec{k}}^{+}(\vec{r})$, we use a plane wave orthogonalized to the individual atomic orbitals $\varphi_\alpha(\vec{r}-\vec{R}_\alpha)$ (here E is the final state energy):

$$\langle f_{\vec{k}}^{+}(\vec{r})| = \langle \vec{k}| - \sum_\alpha \langle \vec{k}|\varphi_\alpha\rangle\langle\varphi_\alpha| \ , \qquad (2.2)$$

rather than to the molecular orbital ψ_i, as has been done previously. These two methods of orthogonalization are not strictly equivalent in the case where $\langle\varphi_\alpha|\varphi_\beta\rangle \neq 0$, which is in fact the case in molecules for φ_α and φ_β on neighboring atoms. However, in the spirit of the present calculation, in which photoionization cross sections in the high photon-energy limit are desired, the φ_α can be chosen to reproduce large $h\nu$ atomic cross sections correctly, but of such a form that overlap corrections to the OPW final state are small.

We now calculate the photoionization transition matrix $\langle\Psi_E|\vec{r}|\psi_i\rangle$. The use of the position operator rather than the momentum operator does not lead to difficulties in the OPW final-state approximation, as origin-dependent terms exactly cancel, as we shall show. Also, we remark that strictly the momentum operator $\vec{P} = -i\hbar\vec{\nabla}$ should be used in the transition matrix, and can be replaced by $\vec{r}$ via the following equation only when ψ_i and Ψ_E are both eigenfunctions of the same Hamiltonian:

$$\langle\Psi_E|\vec{\nabla}|\psi_i\rangle = -(m/\hbar^2)h\nu\langle\Psi_E|\vec{r}|\psi_i\rangle . \qquad (2.3)$$

Since in the OPW approximation we replace Ψ_E by $f_{\vec{k}}^{+}$, which is not an exact solution of the Schrödinger equation for the final-state wave function, Eq. (2.3) is not strictly valid. However, in this case it is not clear whether $\langle f_{\vec{k}}^{+}|\vec{P}|\psi_i\rangle$ or $\langle f_{\vec{k}}^{+}|\vec{r}|\psi_i\rangle$, the "dipole velocity" on the "dipole-length" matrix element is the better approximation. For convenience we chose the latter, in which case the photoionization cross section $d\sigma/d\Omega$ is given by[20,21]

$$\frac{d\sigma}{d\Omega} = \frac{e^2m^2(2mh\nu)^{1/2}}{2\pi mch^4}\, h\nu\,|\hat{A}\cdot\langle f_{\vec{k}}^{+}|\vec{r}|\psi_i\rangle|^2 , \qquad (2.4)$$

where e and m are the electron charge (>0) and mass, c is the speed of light, and $\hat{A}_0$ is the polarization unit vector of the incident light of photon energy $h\nu$.

We now calculate the matrix element of $\vec{r}$ between initial and final states defined by Eqs. (2.1) and (2.2), with the following result:

$$\begin{aligned}\langle\Psi_E|\vec{r}|\psi_i\rangle &= \sum_\alpha C_{i\alpha}e^{i\vec{k}\cdot\vec{R}_\alpha} \\ &\quad\times\left(\vec{q}_\alpha(\vec{k}) - \sum_\beta p_\beta(\vec{k})\rho_{\alpha\beta}\,\delta(\vec{R}_\alpha,\vec{R}_\beta)\right) \\ &= \sum_\alpha C_{i\alpha}e^{i\vec{k}\cdot\vec{R}_\alpha}M_\alpha(\epsilon) \ , \qquad (2.5)\end{aligned}$$

where $\epsilon \equiv k^2$ and

$$\begin{aligned} p_\alpha(\vec{k}) &\equiv \int d^3r\, e^{i\vec{k}\cdot\vec{r}}\varphi_\alpha(\vec{r}) \ , \\ q_\alpha(\vec{k}) &\equiv -i\nabla_{\vec{k}}p_\alpha(\vec{k}) \ , \qquad (2.6) \\ \rho_{\alpha\beta} &\equiv \int d^3r\,\varphi_\alpha(\vec{r})\vec{r}\varphi_\beta(\vec{r}) \ . \end{aligned}$$

In deriving (2.5) individual terms involving orbitals of the form $\varphi_\alpha(\vec{r}-\vec{R}_\alpha)$ were transformed via a change of variables to terms involving $\varphi_\alpha(r)$. In this process, two terms remain (other than the factor $e^{i\vec{k}\cdot\vec{R}_\alpha}$) which explicitly involve the $\vec{R}_\alpha$, and they exactly cancel.[22] In Eq. (2.5) $\delta(\vec{R}_\alpha,\vec{R}_\beta)$ is the delta function and explicitly introduces our approximation of neglecting overlap integrals between orbitals on different atomic sites. The plane-wave formalism is obtained from Eq. (2.5) by simply setting $\rho_{\alpha\beta}$ equal to zero.

We now reiterate our two principal reasons for rederiving the OPW formalism. One reason is that we can use this approximate IAC method to illustrate the use of orbitals other than Slater-type orbitals for the φ_α in Eq. (2.5). Thus, we will explore in Sec. III the use of hydrogenic forms for the φ_α in which we vary the effective value of Z to demonstrate the sensitivity of the gas-phase angular-dependent "β factors" to choice of atomic wave functions. There we will see that the sensitivity of the β factors to the choice of Z helps explain the lack of agreement between previous OPW-based theoretical models and experiment.[23]

Second, the OPW method serves to introduce the more general formulation of the IAC method that we will now discuss in Sec. IIB. In addition, it will serve as an approximate calculation which will nevertheless illustrate general features of the IAC method such as the manner in which the nature of the predicted results changes as one switches between two photon-energy-dependent regimes.

B. Independent-atomic-center approximation

The general expression for the amplitude of a photoelectron of final state energy E at a detector at position $\vec{R}$, when the initial wave function is an atomic orbital $\varphi_\alpha(r)$ centered at the origin is[24]

$$A_\alpha(\vec{R},\epsilon) = \int d^3r\, G_\epsilon(\vec{R},\vec{r})\vec{A}_0\cdot\vec{P}\varphi_\alpha(\vec{r}) \ , \qquad (2.7)$$

where G_ϵ is the propagator for the final state electron in the atomic potential $V(\vec{r})$, ϵ is related to E by $\epsilon = 2mE/\hbar^2$, and A_0 is the nonoscillatory part of the vector potential (dipole approximation).

We will evaluate Eq. (2.7) for the case $|\vec{R}| = R \to \infty$, which assumes a detector far from the

molecule of interest. In this limit a knowledge of the (spherically symmetric) atomic potential $V(r)$ is sufficient for computing $A_\epsilon(\vec{R})$, and requires only numerical integration of the radial Schrödinger equation in the region where $V(r) \neq 0$. We will then generalize the resulting expression to the case where φ_α is not centered at the origin. Summing the resulting amplitude over all atomic orbital components of ψ_i will then lead to the general result for the IAC approximation.

If we define $U(r) = U(|\vec{r}|) = 2mV(r)/\hbar^2$, then we can write a final-state wave function $\psi_k(r)$ (of energy $E_k = h^2k^2/2m$) in the form

$$\psi_k(\vec{r}) = \sum_l f_k^l(r) y_l^m(\hat{r}) , \tag{2.8}$$

where f_k^l is determined from

$$\left(\frac{d^2}{dr^2} + k^2 - U(r) - \frac{l(l+1)}{r^2} \right) f_k^l(r) = 0 . \tag{2.9}$$

The Green's function $G_\epsilon(\vec{R}, \vec{r})$ in Eq. (2.7) is then given by

$$G_\epsilon(\vec{R}, \vec{r}) = \int_0^\infty 2k dk \, \frac{\psi_k(\vec{R}) \psi_k^*(\vec{r})}{\epsilon - k^2 + i\Delta}$$

$$= \sum_{l,m} y_l^m(\hat{R}) y_l^{*m}(\hat{r}) G_\epsilon^l(R, r) , \tag{2.10}$$

where

$$G_\epsilon^l(R, r) \equiv 2 \int_0^\infty k \, dk \, \frac{f_k^l(R) f_k^l(r)}{\epsilon - k^2 + i\Delta} . \tag{2.11}$$

If now the asymptotic form

$$f_k^l(R) \xrightarrow[R \to \infty]{} [(2l+1)/2ikR] \times [(-1)^{l+1} e^{-ikR} + e^{2i\delta_l} e^{ikR}] \tag{2.12}$$

is substituted into (2.11), we find

$$\lim_{R \to \infty} G_\epsilon^l(R, r) = 2\pi(2l+1) \times \begin{Bmatrix} \cos\delta_l \\ i \sin\delta_l \end{Bmatrix} e^{i\delta_l} \frac{e^{ikR}}{kR} f_k^l(r) \tag{2.13}$$

or

$$\lim_{R \to \infty} G_\epsilon(\vec{R}, \vec{r}) = \frac{e^{ikR}}{kR} \sum_l 2\pi(2l+1) \times \begin{Bmatrix} \cos\delta_l \\ i \sin\delta_l \end{Bmatrix} e^{i\delta_l} f_k^l(r) \times \sum_m y_l^m(R) \hat{y}_l^{m*}(\hat{r}) , \tag{2.14}$$

where

$$\begin{Bmatrix} \cos\delta_l \\ i \sin\delta_l \end{Bmatrix} \text{ is used for } \begin{Bmatrix} l \text{ even} \\ l \text{ odd} \end{Bmatrix} .$$

If we define

$$M_{l,\alpha}^m(\epsilon) \equiv \frac{2\pi(2l+1)}{k} \begin{Bmatrix} \cos\delta_l \\ i \sin\delta_l \end{Bmatrix} e^{i\delta_l} \times \int d^3r f_k^l(r) y_l^{m*}(r) \vec{A}_0 \cdot \vec{P} \varphi_\alpha(r) , \tag{2.15}$$

then Eq. (2.7) becomes

$$A_\alpha(\vec{R}, \epsilon) = \frac{e^{ikR}}{R} \sum_{l,m} Y_l^m(\hat{R}) M_{l,\alpha}^m(\epsilon) . \tag{2.16}$$

The determination of $f_k^l(r)$ and $M_{l\alpha}^m(\epsilon)$ will be discussed in the Appendix. Also, we note that $\vec{P}$ in Eq. (2.15) could be replaced by $\vec{r}$ as in Eq (2.3).

We are now in a position to calculate the IAC result for photoemission from a molecular orbital $\psi_i(r)$ given as a sum of atomic orbitals in Eq. (2.1). Our approach is to rewrite Eq. (2.16) for the case where φ_α is centered at $\vec{R}_\alpha$ multiply by $C_{i\alpha}$ [the coefficient of $\varphi_\alpha(\vec{r} - \vec{R}_\alpha)$ in $\psi_i(\vec{r})$ in Eq. (2.1)], and sum over α. When φ_α is centered at $\vec{R}_\alpha$, Eq (2.16) simply gains a phase factor $e^{i\vec{k} \cdot \vec{R}_\alpha}$ where $\vec{k} \equiv k\hat{R}$. This result is derived by realizing that replacing $\vec{r}$ by $\vec{r} - \vec{R}_\alpha$ is equivalent to replacing $\vec{R}$ by $\vec{R} + \vec{R}_\alpha$, and then expanding the result for $|\vec{R} + \vec{R}_\alpha|$ in powers of R_α/R and dropping all higher-order terms.

This procedure results in the final IAC expression for $A_{\text{tot}}(\vec{R}, \epsilon)$:

$$A_{\text{tot}}(\vec{R}, \epsilon) = \frac{e^{ikR}}{R} \sum_\alpha C_{i\alpha} e^{i\vec{k} \cdot \vec{R}_\alpha} \sum_{l,m} M_{l,\alpha}^m(\epsilon) y_l^m(\hat{R})$$

$$= \frac{e^{ikR}}{R} \sum_\alpha C_{i\alpha} e^{i\vec{k} \cdot \vec{R}_\alpha} N_\alpha(\vec{k}) . \tag{2.17}$$

We now emphasize the simple structure of this result, and compare it with the OPW result [Eq. (2.5)]. The first factor in Eq. (2.17) represents the damping and oscillation of the spherical wave emerging from the molecule at large distances, and contains no angular dependence. The sum over α, which gives the angular dependence, is a sum over contributions from individual atomic orbitals. Each contribution is a product of three amplitudes: (i) the amplitude with which φ_α is represented in ψ_i; (ii) the amplitude (phase factor) arising from the extra path length to the detector due to the fact that φ_α is not at the origin; and (ii) the amplitude for optical excitation from an initial orbital φ_α to a final continuum wave function at energy $\hbar^2\epsilon/2m$ (the "atomic factor").

Factors (i) and (ii) are also contained in the OPW result, Eq. (2.5), while factor (iii) is approximated by $M_\alpha(\epsilon)$ in Eq. (2.5). If it were not for the phase factor $e^{i\delta_l}$ in $M_{l,\alpha}^m(\epsilon)$ in Eq. (2.17), then the atomic factor $M_\alpha(\epsilon)$ in the OPW result

could be made to approximate $N_\alpha(\epsilon)$ in Eq. (2.17), the IAC result. This could be done, for example, by making the φ_α variational functions, and adjusting parameters to satisfy some variational principle or, alternatively, to replace the OPW final-state wave function by a plane wave plus an arbitrary combination of φ'_α, with variable coefficients. However, the factors $e^{i\delta_l}$ represent phase factors arising from the effect of the atomic potential on the continuum wave functions. These phase factors are irrevocably lost in the OPW (or plane-wave) approach. In these latter approaches, the final-state wave function is an *ansatz*, and the phase at large distances is fixed from the beginning. This is probably one of the principle reasons for the failure of recent OPW calculations to obtain agreement[17] with experimental results for the angular dependence of photoemission from molecular vapors.[23] Other reasons probably include the use of the OPW approximation near threshold (where contributions from the bonding region are significant and an IAC type of approximation fails), and the use of Slater orbitals for the φ_α, rather than true atomic wave functions.

Finally, a rather important consequence of Eq. (2.17) arises in certain special cases. Namely, if ψ_i is composed predominately of orbitals φ_α which are all of the same type (e.g., C-2p_z orbitals forming one of the high-lying π orbitals of benzene), then $N_\alpha(\vec{k})$ in Eq. (2.17) is the same for all α and factors out of the sum over α. In this case, the factor $\sum C_\alpha e^{i\vec{k}\cdot\vec{R}_\alpha}$ gives in a simple way an angle-dependent function which is usually only slowly modulated by the prefactor $N_\alpha(\vec{k})$. Further, by proper choice of the molecular orientation, light polarization, etc., one can find experimentally important examples where $N_\alpha(\vec{k})$ is a constant, independent of $\vec{k}$, for some path of $\vec{k}$ in the polar coordinate system. An example of such a case will be given in Sec. III, and will provide a demonstration that one can use the IAC formalism in some special but important cases in a very simple way, without the need for calculating the atomic transition matrices $M^m_{l,\alpha}(\epsilon)$.

III. APPLICATIONS OF THE INDEPENDENT-ATOMIC-CENTER FORMALISM

A. OPW and PW angular distributions for oriented CO

The calculation in this section will illustrate two points. One is the transition between the low-energy regime, where individual atomic matrix elements (or angular distributions) dominate, and the high-energy or "structure-factor" regime (see Fig. 2). The second point to be made is

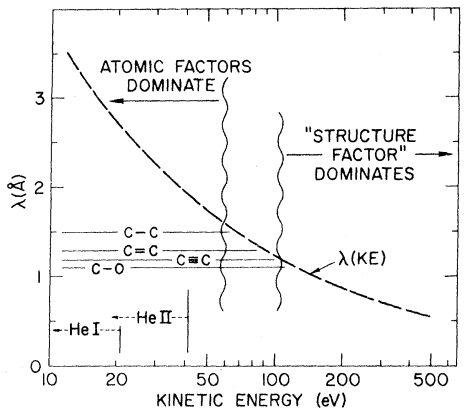

FIG. 2. The final-state electron wavelength is plotted as a function of its kinetic energy and compared with several bond lengths. This comparison graphically illustrates the separation of photoemission into two physical regimes as discussed in the text. For energy $\gtrsim$100 eV one will begin to see a molecular "diffraction pattern," while at the low energies accessible to He resonance lamps, one sees effects due to the atomic transitions alone.

that the OPW and PW approximant lead to very different predictions, especially in the low-energy regime. The implication of this latter fact is that *any* proper calculation—whether or not it includes multiple scattering—should determine the final-state radial atomic functions $f^l_k(r)$ by integrating the Schrödinger equation directly.[24] Performing this rather simple task—straightforward because it consists of integrating only a one-dimensional equation—should lead to much more accurate results for comparison with experiment. However, for some simple geometries the angular distributions are totally independent of the $f^l_k(r)$ (in the case where multiple scattering is neglected) as we will demonstrate by a particular example in Sec. III B.

We implement the OPW formalism described in Sec. II A for the case of CO oriented as shown in Fig. 3(a). The CO molecule lies along the x axis, and unpolarized light is incident in the z

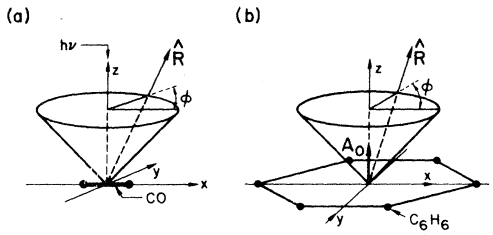

FIG. 3. (a) and (b) illustrate the geometry of emission from oriented CO and benzene, respectively, illustrated in Fig. 4 and 5.

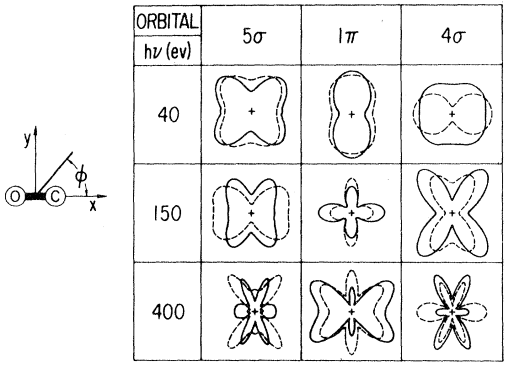

FIG. 4. Polar distributions of emission from CO, oriented as shown in Fig. 3(a), in the plane-wave (dashed) and OPW (solid) approximations. These results are shown for three orbitals of CO, and for three final-state electron energies.

direction. Photoelectrons are collected on a cone of half-angle 45° with its axis along the z direction, and the emitted intensity will be plotted as a function of the azimuthal angle ϕ about this cone. The calculation for the total amplitude is performed independently for light polarization $\vec{A}_0$ parallel to x (which excites only σ orbitals) and parallel to y (which excites only π orbitals). In each case the total amplitude is squared to obtain an intensity, and then the *intensities* are added.

For the initial-state molecular orbitals $\psi_i(\vec{r})$, we have obtained atomic orbital coefficients $C_{i\alpha}$ from a Gaussian-70 calculation using a minimal basis set.[19] For this calculation the resulting $C_{i\alpha}^2$ do not sum to 1 (due to the nonorthogonality of the basis orbitals on neighboring atoms), and the φ_α in the basis set include the 1s core orbitals of C and O, as well as the 2s and 2p orbitals. The core orbital coefficients are quite small and may be neglected for the high-lying (valence) molecular orbitals of interest to us, and the lack of unit normalization can be ignored, since we will present here simply the unnormalized variation of photoemission intensity as a function of ϕ [Figs. 3(a) and 4].

Once the $C_{i\alpha}$ are determined, we replace the Gaussian φ_α basis orbitals of the molecular-orbital calculation by more-realistic atomic orbitals, as discussed previously. We have used here hydrogenic atomic orbitals, with effective core valence Z determined by Slater's prescription.[25] These functions retain the proper node structure of the orbitals, which is an advantage in our calculations, which extend to large values of $h\nu$. However, they do not properly reflect the changing value of Z as a function of r as do true Hartree-Fock atomic orbital calculations (see Appendix). Due to the crudeness of the OPW final state, hydrogenic orbitals are adequate for our present purposes.

The results of OPW (solid) and PW (dashed) calculations for intensity $I(\phi)$ are plotted in polar form in Fig. 4 for the 5σ, 1π, and 4σ orbitals of CO for $h\nu = 40$, 150, and 400 eV. To determine the final-state kinetic energies binding energies were determined from experiment[26] for the case of CO adsorbed on Ni, rather than those obtained from the Gaussian-70 molecular-orbital calculation.

At $h\nu = 40$ eV, in the regime where atomic matrix elements dominate (see Fig. 2), the results for a given orbital can be qualitatively different for the OPW and PW cases (e.g., see the result for the 4σ orbital), and the symmetry of the resulting distributions is different for different orbitals. As expected, in this regime even the symmetry of the resulting pattern is sensitive to both the final-state and initial-state wave functions, and does not represent the geometry of the molecule itself. One also sees here the interesting fact that the asymmetry in the pattern along the C-O axis is extremely slight although present. This result is seen at all photon energies and suggests that measurements of this type may not easily distinguish which end of a linear molecule such as this one lies in a particular direction.

The results for $h\nu = 400$ eV, in the regime where the molecular structure factor dominates (Fig. 2), much more universally reflect the molecular geometry, rather than the details of the initial (e.g., 5σ vs 1π) or final state (OPW vs PW) wave functions. At this high photon energy we see very strongly angle-dependent distributions reminiscent of multicenter diffraction patterns. In all cases (except the 5σ-PW case) one sees a sixfold diffraction pattern, although the orientation of this pattern depends on the initial-state wave-function symmetry through the $C_{i\alpha}$, which act as phase factors which can rotate the pattern. (The 5σ-PW case has eight lobes, due to the particular matrix elements which arise in that case.)

Finally, the $h\nu = 150$-eV distributions are more similar to the 400 eV than the 40 eV distributions as far as their universal shape, irrespective of initial or final wave function, is concerned. This result implies that as the final-state electron wavelength becomes comparable to molecular dimensions (or bond lengths), the diffraction pattern due to the structure factor rather rapidly begins to become evident in the results.

B. Factorization of the total amplitude into atomic and geometric parts

The general formula for the angle-dependent part of the total IAC approximation amplitude, Eq. (2.17)

is a sum of terms, each one containing a geometrical factor $e^{i\vec{k}\cdot\vec{R}_\alpha}$, and an atomic factor $N_\alpha(\vec{k})$. Thus, even for $h\nu$ large, where $e^{i\vec{k}\cdot\vec{R}_\alpha}$ is a strongly varying function of the direction of $\vec{k}$, the relative size of the various $N_\alpha(\vec{k})$ enters into the determination of the final angle-dependent intensity. A great simplification occurs, however, in many cases of interest, for example, photoemission from a particular π orbital ψ_i of a planar hydrocarbon molecule, in which case $C_{i\alpha} \neq 0$ only for atomic orbitals $\varphi_\alpha(\vec{r}-\vec{R}_\alpha)$ of exactly the same chemical and orbital character (in this case C-2p orbitals oriented perpendicular to the plane of the molecules.) In this case the total amplitude becomes

$$A_{\text{tot}}(\vec{R},\epsilon) = \frac{e^{ikR}}{R} N_\alpha(\vec{k}) \sum_\alpha C_\alpha e^{i\vec{k}\cdot\vec{R}} \quad . \tag{3.1}$$

The sum over α in Eq. (3.1) is now extremely simple to compute, and for large $h\nu$ will completely dominate the angular position of maxima and minima in A_{tot}, while $N_\alpha(\vec{k})$ will act only as an "envelope function," modulating the intensity of these features. Thus, in this case the most essential features of the angular distribution needed for molecular orientation determination are found from a simple molecular orbital calculation, which gives the C_α, and from the molecular geometry.

A further simplification can be introduced if, in cases such as have just been discussed, the molecule, energy analyzer, and light polarization are chosen appropriately. In this case the factor $N_\alpha(\vec{k})$ can be made independent of $\hat{k}$, and the angular variation in A_{tot} is *totally* determined by the geometrical and $C_{i\alpha}$-dependent sum

$$A_{\text{tot}}(\vec{R},\epsilon) \propto \sum_\alpha C_{i\alpha} e^{i\vec{k}\cdot\vec{R}_\alpha} \quad . \tag{3.2}$$

An example of this kind, which we now calculate, is the case of benzene oriented as shown in Fig. 3(b) (with the molecular plane perpendicular to the z axis) and the polarization vector A_0 parallel to z. Again we take the collector direction to lie on a cone such that its polar angles are $\theta = 45°$, ϕ variable. For this case all π orbitals are composed only of C-2p_z atomic orbitals and $\vec{k}$ is oriented with respect to these orbitals so that $N_\alpha(\vec{k})$ = constant for all $\vec{k}$ on the photoelectron collection core.

We have calculated the total photoemission intensity versus azimuthal angle ϕ for this case, using Eq. (3.2). For the two highest π orbitals, and photon energies of 40, 100, 200, and 400 eV we plot the resulting angular distributions vs ϕ in Fig. 5. These results show clearly the extent to which the geometric factors contribute something like a "diffraction pattern" for an oriented molecule.

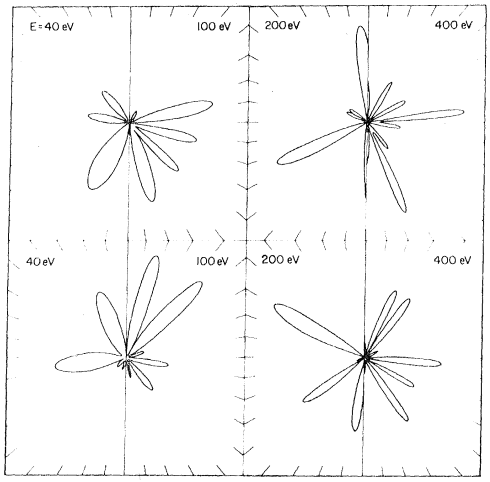

FIG. 5. Emission from oriented benzene [see Fig. 3(b)] for the two highest occupied orbitals, at final state energies of 40, 100, 200, and 400 eV. The top row shows polar plots of emission intensity from the highest-lying π orbital (orbital 21) while the next row shows patterns from the next highest (orbital 20). The 0° origin of each plot is at the top, and corresponds to molecular orientation as shown in Fig. 3(b). Referring to Fig. 3(b), starting with the carbon atom at 0° (on the $+x$ axis), and going counterclockwise in the x-y plane, the atomic p_z orbital coefficients for orbital 21 are 0.27, −0.27, −0.54, −0.27, 0.27, 0.54. Those for orbital 20 are −0.46, −0.46, 0.0, 0.46, 0.46, 0.0.

Due to the lack of any other angular factors, and due to the large size of the molecule, angular variations due to the $e^{i\vec{k}\cdot\vec{R}_\alpha}$ are evident even at the lowest photon energies, although they become much more pronounced and dramatic at large $h\nu$.

Also, the difference between the two π orbitals emphasizes that the angular pattern is not due to a true molecular structure factor of the form $\sum e^{i\vec{k}\cdot\vec{R}_\alpha}$, which depends only on molecular geometry. Rather, in Eq. (3.2) the $C_{i\alpha}$ also enter the sum, so the ultimate angular dependence receives an important contribution from the atomic orbital coefficients $C_{i\alpha}$ composing the molecular orbital of interest.

C. β factors for vapor phase CO

We have calculated the angle-dependent factors for photoemission from vapor-phase CO for both plane-wave and OPW final states, and for various values of the ionic charge Z appearing in the hydrogenic atomic orbitals. The orbital coefficients $C_{i\alpha}$ were obtained as in Sec. III A, but binding energies were adjusted in this case to vapor-phase values.

The quantity of interest here is the factor β appearing in the following formula:

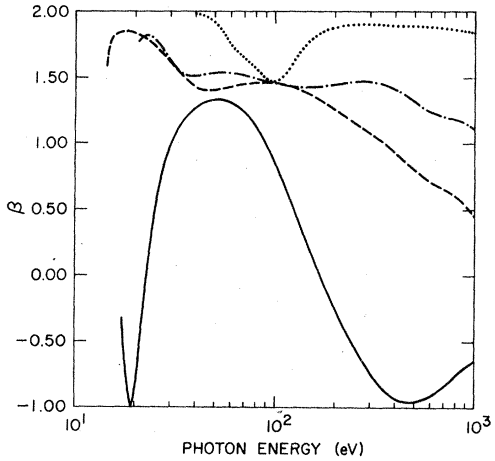

FIG. 6. $\beta(h\nu)$ for vapor-phase CO with an OPW final state, hydrogenic orbitals, and effective Z's obtained by Slater's prescription (Ref. 26). The β values for the 3σ, 4σ, 1π, and 5σ, orbitals are represented by the dotted, dot-dashed, solid, and dashed curves, respectively.

$$I_{\text{tot}}(\theta_{\vec{A}_0,\vec{k}}) \propto 1+\beta P_2(\cos\theta_{\vec{A}_0,\vec{k}}) \qquad (3.3)$$

which gives the total emitted intensity as a function of the angle between the emitted electron wave vector $\vec{k}$ and the light polarization $\vec{A}_0$. It is well known that the only functional form for $I_{\text{tot}}(\theta_{\vec{A}_0,\vec{k}})$ is the one given here, with $\beta(h\nu)$ the parameter uniquely determining the angular distribution of photoemitted electrons from a vapor of a particular chemical species at a particular photon energy.

In Fig. 6 we plot $\beta(h\nu)$ for four molecular orbitals of CO calculated using the OPW final-state

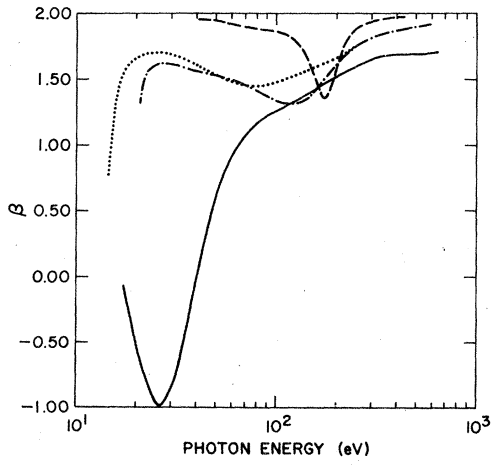

FIG. 7. $\beta(h\nu)$ for CO for a plane-wave final state, hydrogenic orbitals, and Slater Z's. β for the 3σ, 4σ, 1π, and 5σ orbitals is represented by the dashed, dot-dashed, solid, and dotted curves, respectively.

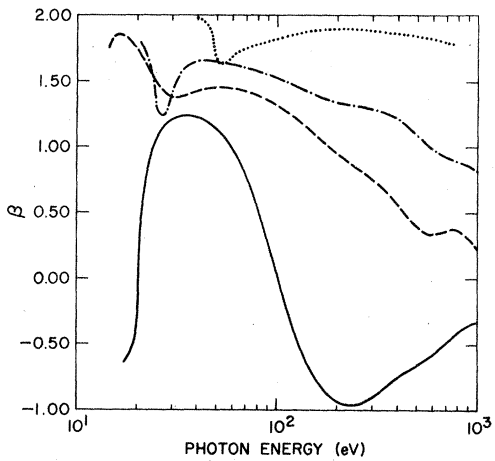

FIG. 8. $\beta(h\nu)$ for CO for an OPW final state with hydrogenic initial-state orbitals, as in Fig. 6, but with effective Z's for the hydrogenic wave functions which are 0.7 times the Slater values. As for Fig. 6, β for the 3σ, 4σ, 1π, and 5σ orbitals is represented by the dotted, dot-dashed, solid, and dashed curves, respectively.

wave function, and Slater's values for Z and C and O for the hydrogenic atomic orbitals. Figure 7 presents the same quantities using a PW final state,[27] while $\beta(h\nu)$ in Fig. 8 used an OPW final state, but the Slater values for Z were scaled down by a factor of 0.8.

The results presented here first of all show the difficulty of calculating $h\nu = 21.2$ eV β factors which agree with experiment. While Refs. 1–6 have attempted such calculations, we see that the results at 21.2 eV are extremely sensitive to the approximations one makes, due to the rapid variation of $\beta(h\nu)$ in this energy range. This point was also realized by the authors of Refs. 1–6. Additionally, atomic resonances of various types appear here,[18] near threshold, further complicating the physical phenomena determining the β factors. We feel, based on these results, that it is possible that in cases where atomic resonances are not important, proper application of the IAC *may* be capable of correctly yielding β factors at $h\nu = 21.2$ eV. However, this possibility remains to be demonstrated. It may be necessary in this regime to include intramolecular multiple scattering to some order, since in this energy range one expects rather large values for the atomic t matrix at large angles. We emphasize that our intent in this paper is to consider the IAC approximation as one which is valid in a high-energy limit, and attempts to extend it to low energies may fail.

At high photon energies, Figs. 6–8 illustrate a

large variety of structure in $\beta(h\nu)$. This structure comes both from the nodes in the φ_α which we have made qualitatively correct by using hydrogenic wave functions, and from spherical Bessel functions in the ensemble average of Eq. (2.5), which describe interference between atomic centers. These geometry-based interference terms are thus evident in vapor phase $\beta(h\nu)$ at large $h\nu$ for the same reasons they are seen in Figs. 4 and 5 at large $h\nu$, but in the vapor-phase case their manifestation is seen in a different measured quantity.

Finally, we learn from Figs. 6–8 that even at large values of $h\nu$, the dependence of β on photon energy is very different for the OPW and PW case.[27] This is in contrast to the large $h\nu$ oriented-molecule angular distributions (Fig. 5), which at large $h\nu$ tend to show a predominately geometry-dependent "diffraction pattern" for the molecule. This contrast is due to the fact that for large $h\nu$ the atomic factors tend to modulate lobe intensities in the oriented-molecule emission patterns, but do not usually change the angular position of maxima and minima. However, $\beta(h\nu)$ is apparently very sensitive to such modulation. For this reason, comparison of calculated values for $\beta(h\nu)$ with experimental values over a wide energy range using synchrotron radiation will constitute a strong test of the theoretical calculation. The converse implication is that even an approximate IAC-based theory may be adequate for calculating angular distributions from oriented molecules at a fixed photon energy.

IV. DISCUSSION

The present section reemphasizes three major features of the IAC approximation which were developed in the preceding sections. These are listed here and then will be discussed individually:

(i) At large $h\nu$, when multiple scattering is not dominant,[28-31] geometrical and atomic angular factors contribute to the total angle-dependent intensity in different ways, which can be separated.

(ii) The present development of the IAC shows how one may improve greatly on the OPW and PW approximations, and may permit vapor-phase β factors to be calculated well enough to permit their use in the interpretation of vapor-phase photoemission spectra.

(iii) The IAC approximation provides a starting point for the calculation of multiple scattering, as it provides a simple form for the initial state needed at the start of any multiple-scattering calculation.

The first feature listed above has been discussed in detail already. We emphasize that the use of geometrical information can be extracted from large $h\nu$ molecular angular distributions in two ways. In the general case, the simplest approach is to use the position (angular separation) of sharp lobes in the angular distribution to identify the geometrical information in Eq. (2.17). That is, one can ignore the modulation of lobe intensity (and possible rotation of the pattern by atomic factor phases) and simply use the sharp structure as a guide. With more effort, one can integrate the Schrödinger equation for the final-state atomic functions—a procedure which is relatively simple due to the spherical potential and availability of analytic approximations to the initial atomic states and charge densities.[32] Such a calculation then yields the atomic factors in Eq. (2.17) so that a more detailed comparison of theory and experiment can be made. We also showed that by judiciously choosing detector and light-polarization directions, the atomic factors can be made to disappear completely from the problem for many important cases involving symmetric hydrocarbon molecules. In such a case it is a *rigorous* feature of the IAC formulas that the atomic factors can be completely ignored, and only the simple "geometrical" factor calculated (see Sec. III B). It was also shown in Sec. III B that for such molecules, even in the more general case where the atomic factors do not disappear completely, they become one simple prefactor in front of the "geometrical" sum, so that they do not change the position of geometry-induced lobe positions.

The second major feature of our paper is that it shows that the IAC formula (2.17) is of the same *form* as the often used OPW result [Eq. (2.5)]. Since the IAC result also provides a well-defined prescription for calculating the atomic transition amplitudes, it provides a natural extension of the previous models based on the OPW approximation. In particular, Eq. (2.17) shows that the phase shift accrued by the final-state electron as it leaves an atomic potential properly enters the IAC formula, while the phase at large distances is simply fixed in an *ad hoc* way in the OPW formulation. This phase problem, as well as improper atomic amplitudes, may be one of the reasons for the failure of the OPW approach to properly predict vapor-phase β factors, and the IAC method might improve on the calculation of such factors. However, we feel that such a program will have most success if β factors are measured at large values of $h\nu \geq 100$ eV (e.g., using synchrotron radiation). For the many measurements available at $h\nu = 21.2$ eV using He discharge light sources, intramolecular multiple scattering is likely to contribute strongly.

Finally, the IAC results we present here provide a starting point for an intramolecular as well as a

substrate multiple-scattering calculation. As the wave leaving the molecule in the IAC approximation is a sum of independent (but coherent) spherical waves, each such wave can be used as the incident wave in a calculation of multiple scattering from the substrate based on one of the many LEED-type calculations now available. Intramolecular scattering (and substrate scattering as well, as an alternative to a LEED-based calculation) can also proceed via a sum over real space propagations between scattering centers, similar to some calculations of EXAFS.[28-31] There are indications in the literature (e.g., Ref. 28–31) that terminating such a calculation after including scattering only to a rather low order may be justified in the particular case treated here. The important point is that the initial wave here is spherical, not a plane wave as in the LEED case, and Lee[28-31] has shown that in this case multiple scattering need not necessarily be carried out to the high order required for LEED. Also, we are *not* interested in calculating intensity versus $h\nu$ (as was done, for example, by Leibsh[6]), but rather intensity versus detector angle at fixed $h\nu$. This important difference also may contribute to the success of a calculation based on multiple scattering only to a low order (one or two scattering event terms), for after many scatterings (which may still contribute to the angle integrated intensity), sharp angular structure, due for example to the symmetry of the adsorption site, probably disappears from the result.

ACKNOWLEDGMENTS

Special thanks are due to J. W. Davenport, who provided many stimulating discussions and a critical review of the manuscript. I also wish to acknowledge useful discussions with J. Demuth, D. E. Eastman, P. Feibelman, J. Freeouf, D. Jepsen, P. Lee, K. Pandey, G. Rubloff, and A. Williams.

APPENDIX

The main point of this Appendix is to show that the most central problem in calculating the angle-dependent photoemission from molecules—namely, the accurate determination of the final-state wave function—is made tractable in the IAC approximation. The most intractable part of the problem of finding the final-state wave function, the multicenter nature of the molecule, is eliminated in the IAC approximation by the decomposition of the total transition matrix into a sum of individual terms each of which contains a matrix element [see Eqs. (2.15) and (2.16)] between an atomic eigenfunction φ_α and a solution of the Schrödinger equation, $f_k^l(r)y_l^m{}^*(\hat{r})$, in an atomic potential at final state energy $E_k=\hbar^2k^2/2m$. Once the atomic potential $U(r)$ of Eq. (2.9) is determined, one can numerically integrate (2.9) to determine $f_k^l(r)$ up to a multiplicative normalization factor, which is then determined by matching the solution of Eq. (2.9) to the asymptotic form of f_k^l given in (2.12).

The two most physically significant questions that arise in implementing this procedure are the following: (i) Since $f_k^l(r)$ is needed near the atomic core for calculating photoemission transition amplitudes at large $h\nu$, how does one easily get the correct multielectron atomic potential $U(r)$ for $r\to 0$? (ii) As the final molecular state is an ionized one, what is the charge state of the molecule used to obtain $U(r)$?

The first question emphasizes the fact that oscillations in $f_k^l(r)$ near $r=0$ contribute strongly to $A_{\text{tot}}(\hat{R})$ at large final energy, so that a $U(r)$ obtained for example from a proper multielectron calculation of the atom is needed in Eq. (2.9) rather than a U(r) based simply on occupied Slater-type orbitals, which have the correct form in the bond region, but not in the atomic core region.

Concerning the charge state of the molecule, one procedure of value would be to perform calculations of $U(r)$ for individual atomic centers in both the neutral and ionized molecules, and compare the results. For large molecules in the vapor phase, ionization of the molecule typically removes only a small fraction of an electron charge from any particular atomic center, so that the result should not be very sensitive to the charge state of the molecule. For the case of molecules on a solid surface, the charge removed from the molecule could be replaced by charge flow from the solid in a time comparable to the photoexcitation time scale, so that the neutral molecule-charge distribution is probably the most sensible one to choose.

In light of the above discussion, we feel that a well-defined reasonable procedure for finding $U_A(r)$ on atom A located at position $\vec{\mathrm{R}}_A$ is the following. One first determines the $C_{i\alpha}$ of Eq. (2.1) for all *occupied* molecular orbitals ψ_i using a standard molecular calculation (Gaussian-70), CNDO-2, etc.) based on Slater-type orbitals, Gaussian orbitals, etc., for the $\varphi_\alpha(\vec{\mathrm{r}}-\vec{\mathrm{R}}_\alpha)$. Then the charge density on atom A $\rho_A(\vec{\mathrm{r}})$ is determined from

$$\rho_A(\vec{\mathrm{r}})=\sum_i \sum_{\alpha,\beta} C_{i\alpha}C_{i\beta}\varphi_\alpha(\vec{\mathrm{r}}-\vec{\mathrm{R}}_\alpha)\varphi_\beta(\vec{\mathrm{r}}-\vec{\mathrm{R}}_\beta) \times \delta_{R_\alpha,R_A}\delta_{R_\beta,R_A}, \tag{A1}$$

where the δ functions imply that charge density on

atom A receives no contribution from neighboring atoms. This assumption neglects bond charge contributions and leaves that part of the charge on an atom near the core region, which contributes most strongly in the region of interest for high-energy photoemission (i.e., in the region in which $\rho_A(r)$ is approximately spherically symmetric about R_A).

While the $C_{i\alpha}$ in Eq. (A1) are determined from a molecular orbital calculation, the φ_α used in that calculation *must* be replced by a good representation of Hartree-Fock wave functions as emphasized previously. This problem is rather straightforward to solve, for there now exist excellent representations of Hartree-Fock atomic orbitals in terms of a finite sum of simple functions. For example, Clementi and Roetti[33] have tabulated representations of the atomic orbitals φ_α as a finite sum of functions of the form $r^n e^{-\alpha r} y_{lm}(r)$. This simple representation of the φ_α can then be used to determine $U_A(r)$ from $\rho_A(r)$ in terms of a sum of a Coulomb potential [obtained from $p_A(r)$ using Poisson's equation] and an effective (one-electron) exchange potential $\{$proportional to $[\rho_A(r)]^{1/3}\}$.

The combination of easily used molecular orbital calculations for finding $C_{i\alpha}$ and simple forms for Hartree-Fock atomic functions φ_α thus makes simple the determination of a rather accurate form for $U_A(r)$ near the atomic core in a molecule, so that direct numerical integration of Eq. (2.9) can be easily carried out. Thus, in a straightforward and simple way the IAC approximation permits a much more accurate calculation of photoionization oscillator strengths and angular distributions far above threshold than can be carried out using the rather crude plane-wave or OPW final-state approximations.

---

[1]F. O. Ellison, J. Chem. Phys. 61, 507 (1974).

[2]J. W. Rabalais, T. P. Debies, J. L. Berkosky, J-T. J. Huang, and F. O. Ellison, J. Chem. Phys. 61, 516 (1974).

[3]J. W. Rabalais, T. P. Debies, J. L. Berkosky, J-T. J. Huang, and F. O. Ellison, J. Chem. Phys. 61, 529 (1974).

[4]T. P. Debies and J. W. Rabalais, J. Am. Chem. Soc. 97, 3 (1975).

[5]B. Ritchie, J. Chem. Phys. 60, 898 (1974).

[6]B. Ritchie, J. Chem. Phys. 61, 3279 (1974).

[7]See, for example, J. E. Demuth, P. M. Marcus, and D. W. Jepson, Phys. Rev. B 11, 1460 (1975).

[8]J. W. Gadzuk, Phys. Rev. B 10, 5030 (1974).

[9]A. Liebsch, Phys. Rev. Lett. 32, 1203 (1974).

[10]A. Liebsch and E. W. Plummer, Faraday Discuss. Chem. Soc. 58, 19 (1974).

[11]J. B. Pendry, J. Phys. C 8, 2413 (1975).

[12]T. B. Grimley and G. F. Bernasconi, J. Phys. C 8, 2423 (1975).

[13]A. Liebsch, Phys. Rev. B 13, 544 (1976).

[14]There are by now a substantial number of papers that demonstrate this point. We refer here to one of the first, namely, J. E. Demuth and D. E. Eastman, Phys. Rev. Lett. 32, 1123 (1974).

[15]A. Liebsch, Phys. Rev. Lett. 32, 1203 (1974).

[16]A. Liebsch, Phys. Rev. Lett. 38, 248 (1977).

[17]The extreme importance of atomic phase shifts in LEED calculations is well known. They are essential for obtaining the correct wave function.

[18]J. W. Davenport, Phys. Rev. Lett. 36, 945 (1976).

[19]W. J. Hehre and J. A. Pople, Gaussian 70, Quantum Chem. Program Exchange, Bloomington, Indiana (unpublished).

[20]L. L. Lohr, Jr., in *Electron Spectroscopy: Proceedings of the International Conference on Electron Spectroscopy*, edited by D. A. Shirley (North-Holland, Amsterdam, 1972), pp. 245–258.

[21]L. L. Lohr and M. B. Robin, J. Am. Chem. Soc. 92, 7241 (1970).

[22]One reason for noting this fact is that it has occurred to us to generalize the OPW final state in Eq. (2.2) to the form $\langle f_{\vec{k}}^{-} | = \langle \vec{k} | - \Sigma B_\alpha \langle \varphi_\alpha |$, and treat the B_α as variational coefficients in some convenient variational formalism such as that due to W. Kohn [Phys. Rev. 74, 1763 (1948)]. However, use of this form with B_α arbitrary leads to terms which depend on the R_α which do not cancel. The cancellation is a particular property of the OPW formalism, in which $B_\alpha = \langle k | \varphi_\alpha \rangle$.

[23]For example, compare typical experimental results for $\beta(h\nu)$ as given in the following reference with results from Ref. 1: T. A. Carlson, G. E. McGuire, A. E. Jonas, K. L. Cheng, C. P. Anderson, C. C. Lu, and B. P. Pullen, in *Electron Spectroscopy: Proceedings of the International Conference on Electron Spectroscopy*, edited by D. A. Shirley (North-Holland, Amsterdam, 1972), pp. 207–231.

[24]I. Adawi, Phys. Rev. 134, A788 (1964).

[25]J. C. Slater, Phys. Rev. 36, 57 (1930).

[26]D. E. Eastman and J. E. Demuth, J. Appl. Phys. Suppl. 2, 827 (1974).

[27]It is well known that $\beta(h\nu)$ is identically equal to 2 for a plane-wave final state if the momentum operator is used in calculating the transition matrix element. This result is obtained by operating on the final-state plane wave with the gradient operator and then showing the the remaining quantity, the *Fourier* transform of the molecular wave function, gives an emission-angle-independent result when averaged over all orientations of the molecule. Our present results in Fig. 8 are not equal to 2 due to our use of the position operator in the transition matrix. As photon energy increases toward 1 keV, our results for β in Fig. 8 approach 2, implying that at these high energies the plane-wave final state begins to reasonably approximate the true final-state wave function, which is the requirement for the validity of replacement of the gradient operator with the position operator in the transition matrix element. This result is in agreement with a calculation by Gottfried [K. Gottfried, *Quantum Mechanics*

(Benjamin, New York, 1966), Chap. 58] for hydrogen in which he shows that at $h\nu$ greater than about several thousand eV the plane-wave approximation for the photoionization final state is a reasonable one.
[28]P. A. Lee and G. Beni, Phys. Rev. B 15, 2862 (1977).
[29]C. A. Ashley and S. Doniach, Phys. Rev. B 11, 1279 (1975).
[30]P. A. Lee and J. B. Pendry, Phys. Rev. B 11, 2795 (1975).
[31]B. M. Kincaid and P. Eisenberger, Phys. Rev. Lett. 34, 1362 (1975).
[32]E. Clementi and C. Roetti, At. Data Nucl. Data Tables 14, 177 (1974).